Influence of the cardiac cycle on velocity selective and acceleration selective arterial spin labeling

Franklin, S.L.; Schmid, S.; Bos, C.; Osch, M.J.P. van

Received: 5 April 2019 | Revised: 3 August 2019 | Accepted: 6 August 2019

DOI: 10.1002/mrm.27973

FULL PAPER

Magnetic Resonance in Medicine

Influence of the cardiac cycle on velocity selective and acceleration selective arterial spin labeling

Suzanne L. Franklin[1,2,3] | **Sophie Schmid**[1,3] | **Clemens Bos**[2] | **Matthias J. P. van Osch**[1,3]

[1]Department of Radiology, C.J. Gorter Center for High Field MRI, Leiden University Medical Center, Leiden, The Netherlands

[2]Center for Image Sciences, University Medical Centre Utrecht, Utrecht, The Netherlands

[3]Leiden Institute for Brain and Cognition, Leiden University, Leiden, The Netherlands

Correspondence
Suzanne L. Franklin, Albinusdreef 2, Leiden, Zuid-Holland 2300 RC, Netherlands.
Email: s.l.franklin@lumc.nl

Funding information
This work is part of the research programmes Drag 'n Drop ASL with project number 14951, and Innovational Research Incentives Scheme Vici with project number 016.160.351, which are (partly) financed by the Netherlands Organisation for Scientific Research (NWO).

Purpose: In this study, the influence of the cardiac cycle on the amount of label produced by a velocity-selective (VSASL) and acceleration-selective arterial spin labeling (AccASL) module was investigated.

Methods: A short-PLD sequence was developed where a single VSASL- or AccASL-module was preceded by pCASL labeling to isolate the arterial blood pool. ASL subtraction was performed with label/control images with similar cardiac phase and time-of-measurement, followed by retrospective binning in 10 cardiac phase bins. ASL signal variation over the heart cycle was evaluated and tested for significance using a permutation test.

Results: VSASL and AccASL showed significant arterial signal fluctuations over the cardiac cycle of up to ~36% and ~64%, respectively, mainly in areas containing large arteries. pCASL also showed significant signal fluctuations, of up to ~25% in arteries. Raw label/control images confirmed that the observed signal fluctuations were caused by the amount of label produced during the cardiac cycle, rather than inflow-effects, because the raw images did not all show equal cardiac phase dependence.
No significant effects of the cardiac cycle were found on the gray matter ASL-signal.

Conclusion: Significant influence of the cardiac cycle on the generated label was found for spatially nonselective ASL-sequences. Hence, to become independent of the cardiac cycle, sufficient averages need to be taken. Alternatively, these findings could be highly interesting for the purpose of quantifying pulsatility more distally in the vascular tree.

KEYWORDS
acceleration-selective arterial spin labeling (ASL), cardiac cycle, perfusion, velocity-selective ASL

1 | INTRODUCTION

Arterial spin labeling (ASL) is a noninvasive MRI technique allowing quantitative perfusion measurements by magnetically labeling arterial blood. In traditional ASL, blood proximal to the imaging volume is magnetically altered in the label image, followed by a post-labeling-delay (PLD) where the labeled blood flows into the imaging region. By

subtracting this label image from a control image in which the inflowing magnetization is unaltered, static tissue signal is removed and only perfusion signal is left.

However, in traditional ASL transit delay artifacts can arise when not all of the labeled blood has reached the imaging volume during the PLD, thereby leading to underestimation of the perfusion and occurrence of vascular artifacts. In velocity-selective (VSASL) and acceleration-selective (AccASL) ASL, blood is not labeled based on location, but based on flow velocity and acceleration, respectively. This suggests that labeling is also performed within the imaging volume, thereby reducing tissue transit-delay artifacts.[1] The VSASL-module creates label by saturating spins above a certain cutoff velocity,[1] or in case of Fourier-transform based velocity selective inversion, inverting spins below the cutoff velocity.[2] The AccASL-module creates label by saturating spins above a certain cutoff acceleration/deceleration.[3] By labeling closer to the target region, VSASL and AccASL offer not only advantages in patients with slow-flow, but also in functional MRI (fMRI) experiments where ASL is used as readout.[4,5]

However, because velocity and acceleration of blood varies over the cardiac cycle, it is our hypothesis that the amount of label generated will depend on the cardiac phase in which the VSASL- or AccASL-module is applied. Previously, the cardiac cycle has already been shown to influence signal stability in other ASL techniques, such as pulsed-ASL[6,7] and pCASL.[8] Inflow of fresh blood[8] as well as transit time[6,7] have been mentioned as mechanisms through which the cardiac cycle influences signal stability. In case of VSASL and AccASL, it is important to know whether the cardiac cycle has a significant effect on the amount of label that is generated to allow correct quantification and interpretation of these techniques, as well as to maximize temporal SNR, which can be considered especially important for functional applications.[4] In the current study, the effect of the cardiac cycle on the amount of label that is produced is examined by using only a *single* VSASL(AccASL)-module with a short PLD, in combination with pCASL prepulse to limit the saturation-effect of the VSASL- and AccASL-modules to *arterial* blood, thereby avoiding contamination by venous signal.

In summary, the aim of this study is to investigate whether the amount of label generated by a VSASL- or AccASL-module depends on the cardiac phase during which the labeling takes place.

2 | METHODS

2.1 | General approach

Both VSASL- and AccASL-modules consist of motion sensitizing gradients, which are switched-on in label condition and switched-off in control condition. The VSASL gradients have alternating polarity, creating label by saturating spins above a certain cutoff velocity, whereas the AccASL gradients all have a positive polarity resulting in saturation above an acceleration threshold. Subtracting label from control thus generates signal from the saturated spins, i.e., the spins above the cutoff velocity (acceleration).

The original VSASL-sequence consists of 2 VSASL-modules with the same cutoff velocity: the first module is either in label or control condition, whereas the second module is played out after a PLD of 1-2 s and is always in label (velocity crushing) condition. The purpose of the second module is to provide a well-defined end to the bolus, enabling quantification, and to remove the venous component of the VSASL signal. The original AccASL implementation consists of only a single AccASL-module, because it inherently has very limited venous labeling.[3]

To study the influence of the cardiac cycle it is important to be able to control the timing of labeling with respect to the cardiac cycle. This means that the effects of a *single* VSASL(AccASL)-module on the arterial blood pool need to be isolated. However, using only a single VSASL-module would result in a mixture of arterial and venous signal and, because arterial and venous systems overlap at tissue level, it would be very hard to isolate the labeled arterial blood using an arterial or venous mask. Therefore, a pCASL-preparation was used to first isolate the arterial signal, which was subsequently saturated by the spatial nonselective single VSASL(AccASL)-module, see Figure 1. Before adopting this experimental design, we also used the same approach in a prospectively triggered manner, see Supporting Information Figure S1, which is available online. The prospectively triggered sequence had a very long pCASL-labeling duration (>7 s), to become insensitive to differences in labeling duration. However, results of this approach were inconclusive, see Supporting Information Figures S2 and S3. Details of the methods and results of this experiment are reported in the Supporting Information.

Combining pCASL and a single VSASL- or a AccASL-module in 1 sequence yields 4 control/label conditions, because both the pCASL- and VSASL(AccASL)-module can be in label or control condition, see Figure 1B. Our main parameters of interest are VSArt and AccArt, see Figure 1C, which represent the amount of pCASL label, i.e., arterial blood, that is saturated by the VSASL- or AccASL-module. VSArt and AccArt are calculated by subtracting the pCASL image with VSASL- or AccASL-crushing from a regular pCASL image. Other possible subtractions and their interpretations, are described in Figure 1C. Whereas our analysis focuses on VSArt and AccArt-images as a function of cardiac phase, single-VSASL(AccASL) images will also be shown to allow evaluation of the effectiveness of the pCASL prepulse to isolate the arterial blood pool, nevertheless it should be noted that the single-VSASL(AccASL)-image will partially contain venous signal. In addition, the pCASL images will be shown to provide information on cardiac phase dependence of label generation by pCASL.

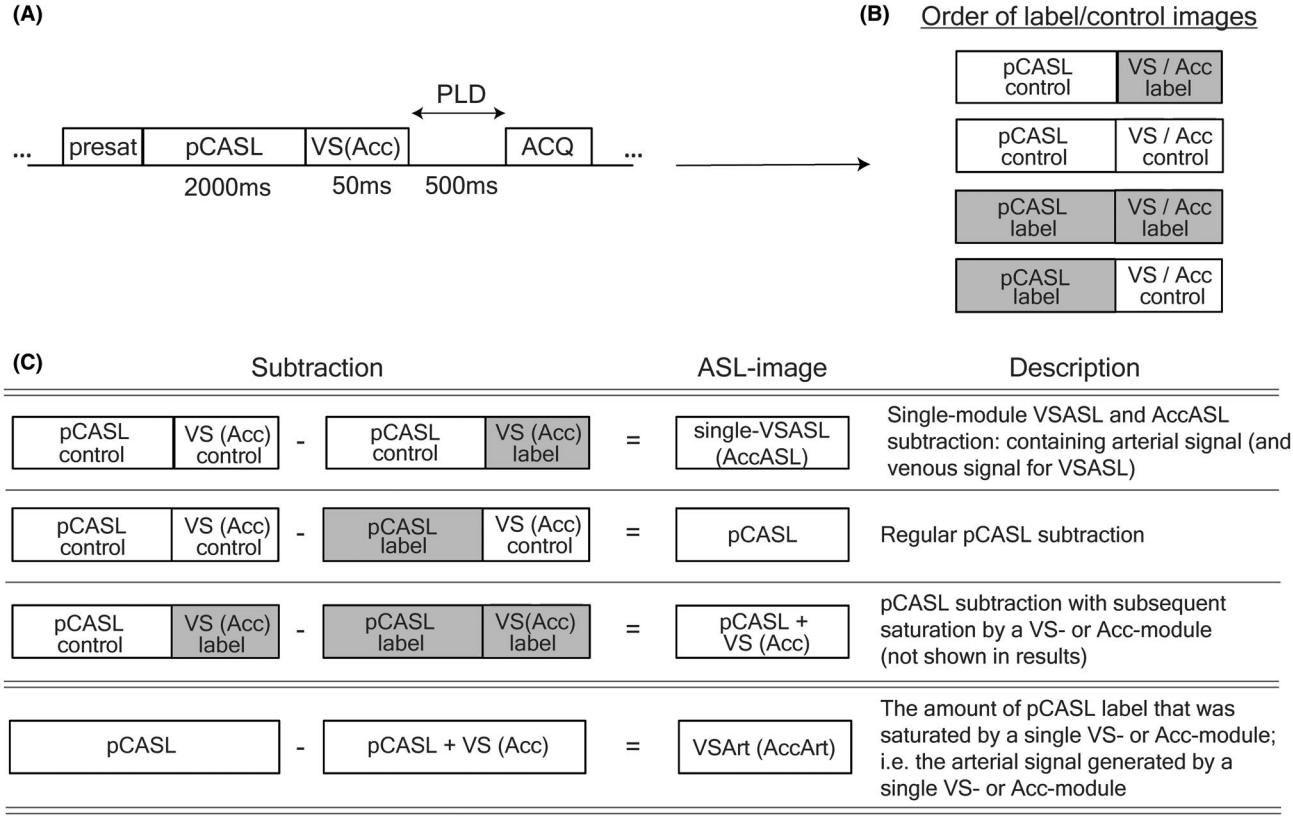

FIGURE 1 A, Sequence diagram for the scans combining pCASL and a VSASL- or AccASL-module. B, Order of label/control conditions for 4 consecutive acquisitions, this was repeated 200 times. C, Subtractions of the label/control images and their descriptions

2.2 | In vivo experiments

In total, 14 healthy volunteers were scanned, 7 (aged, 22-56 years; 3 men and 4 women) with pCASL-VSASL, and 7 (aged, 19-59 years; 3 men and 4 women) with pCASL-AccASL. All volunteers were screened for MRI contra-indications, and provided written informed consent. Cardiac phase was recorded continuously using a peripheral pulse unit (PPU) on the finger of the volunteer. A PPU-triggered phase-contrast quantitative flow scan, planned on the internal carotid arteries (at the location of the pCASL labeling), was acquired to measure blood flow velocity as a function of cardiac phase and to be able to measure the delay in occurrence of the R-peak as measured by PPU and maximum velocity at labeling location. For postprocessing, a 3D T_1-weighted scan was acquired to obtain a gray matter mask, and a whole-brain phase-contrast angiography (PCA) scan was acquired to allow the generation of an arterial mask.

2.3 | MRI acquisition parameters

Scans were acquired on a Philips 3T MRI scanner (Ingenia CX, Philips, Best, The Netherlands) using a multi-slice single-shot EPI readout and a 32-channel head coil.

The ASL scans were acquired with a TR/TE of 3204 ms/16 ms, and 200 repetitions per label/control condition, resulting in a total scan time of 43 min. Presaturation of the imaging region was used before pCASL-labeling using a WET-pulse.[9] The labeling duration of pCASL was set to 2000 ms, which is longer than the average tissue arrival time[10] to make sure that pCASL-signal filled the whole arterial side of the vasculature and to minimize any influence of the cardiac cycle on the distance that label will travel into the (micro)vasculature. The VSASL cutoff velocity was set to 1.9 cm/s and the AccASL cutoff acceleration to 1.3 m/s^2. Background suppression pulses were applied during pCASL labeling at 50 and 1150 ms. See Table 1 for all scan parameters. A relatively short PLD of 500 ms was chosen to reduce cardiac phase dependent effects on the transport of label, i.e., transit delay, as well as cardiac phase dependent inflow from "fresh" spins that did not experience presaturation, while still ensuring enough time for VSASL(AccASL)-gradient induced eddy currents to decay.

The phase-contrast quantitative flow measurement was PPU-triggered and acquired using a single slice 2D-FFE readout, with a TR/TE of 13/8.0 ms, retrospectively reconstructed in 15 heart-phases, with voxels sizes of 0.6/0.6/6 mm, and a phase-contrast encoding velocity of 200 cm/s, resulting in a total scan duration of 2 min 57 s. In addition, a whole-brain PCA scan was acquired using a 3D-FFE readout, with a TR/TE of 20/4.0 ms, reconstructed voxel sizes of 1.1/1.1/1.75 mm,

TABLE 1 Scan parameters for the retrospectively triggered ASL scans

Parameter	ASL scans	
Voxel size	$3 \times 3 \times 7$ mm^3	
Number of slices	17	
TR	3204 ms	
TE	16 ms	
Number of repetitions	200 (per label/control condition)	
Background suppression pulses	50/1150 ms	
Total scan time	43 min	
Post-labeling delay	500 ms	
pCASL labeling duration	2000 ms	
	VSASL	**AccASL**
Labeling module duration	50 ms	50 ms
Gradient duration	0.8 ms	0.8 ms
Gradient strength	17 mT/m	30 mT/m
Cutoff velocity/acceleration	1.9 cm/s	1.3 m/s^2

and a phase-contrast encoding velocity of 30 cm/s, resulting in a total scan duration of 53 s. The 3D-T_1w scan was acquired using a multi-shot 3D-TFE readout, with a TR/TE of 9.7/4.6 ms, using reconstructed voxel sizes of 0.9/0.9/1.2 mm, resulting in a total scan duration of 4 min 57 s.

2.4 | Postprocessing

ASL images were realigned (SPM 12, University College London, London, United Kingdom) and data analysis was conducted using MATLAB R2015b (The MathWorks, Inc., Natick, MA). In regular ASL, label and control images are acquired in an interleaved manner to prevent subtraction errors arising from scanner drift. In the current study, not only scanner drift but also cardiac phase needed to be taken into account. Because the 4 label/control images were not triggered on cardiac phase, no predefined, sequentially acquired label-control pairs with the same cardiac phase were available for subtraction. Thus, images with similar times of measurement as well as cardiac phase needed to be found to perform the subtractions. Suitable images for subtraction were created by performing Gaussian-weighted averaging within the "time-of-measurement/cardiac phase"-plane, see Figure 2. A Gaussian kernel was moved over the plane with a step size of $\pi/5$ in cardiac phase direction and 36*TR in time-of-measurement direction, to obtain a grid of 22×10 data points for each label/control condition. The Gaussian kernel was designed such that it had a full-width-half-maximum of a step size, leading to blurring of half a step size in both directions; 18° (i.e., $\pi/10$) in cardiac phase direction and 18*TR = 58 s in time-of-measurement direction. Subtractions between the label/control conditions were performed per grid point, and then averaged per cardiac phase bin.

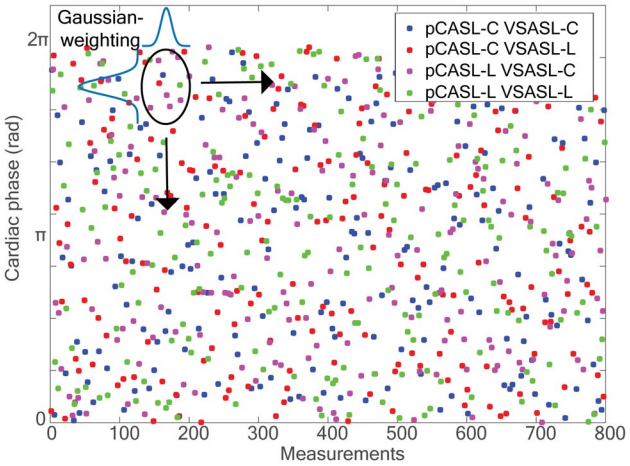

FIGURE 2 Averaging of the raw label/control images for the retrospectively triggered scans to obtain suitable subtraction of images with similar time-of-measurement and cardiac phase, to prevent subtraction errors from scanner drift and cardiac phase differences. Graph shows all the data points acquired in a single scan session. Four different raw images were acquired: $pCASL_{control}$/$pCASL_{label}$ followed by either $VSASL_{control}$ or $VSASL_{label}$. The plot shows how a Gaussian-weighted average was taken of each of the 4 label/control conditions within the ellipse, which was moved over the "measurement time-cardiac phase" plane in 22 steps in time-of-measurement direction, and 10 in cardiac phase direction, to obtain a grid of 22×10 data-points for each label/control condition. Subtractions of the label/control conditions were performed per grid-point. Lastly, the data were averaged per cardiac phase bin

Arterial and gray matter masks were generated to be able to obtain separate gray matter and arterial signal curves. To this end, the pCASL image was co-registered separately to the T_1-based gray matter segmentation and the whole-brain

PCA scan. The inverse transformation matrix was consequently applied to, respectively, the T_1-based gray matter segmentation and PCA scan, which were then both reformatted to the same space and resolution as the ASL images (all performed in SPM12). A vascular mask was generated by thresholding of the whole-brain PCA scan. Next, an arterial mask was generated by selecting only those voxels in the vascular mask that had an intensity above a manually determined threshold on the mean pCASL image. A gray matter mask was generated by segmenting the 3D T1-weighted scan (SPM12). Lastly, voxels from the gray matter segmentation that were also part of the vascular mask were removed. The arterial and gray matter mask were used to generate separate arterial and gray matter signal intensity curves of all ASL images as a function of cardiac phase.

The phase-contrast quantitative flow scan provided blood flow velocity curves over the cardiac cycle relative to the moment of PPU-trigger detection, allowing temporal alignment of label generation to the cardiac cycle and corresponding blood flow velocities. From the PPU-triggered phase-contrast quantitative flow scan, the delay in occurrence of the R-peak measured by the PPU and maximum velocity at the pCASL-labeling location, was calculated. The R-peak delay was used to correct the cardiac phase of the blood flow velocity curves as well as the ASL data points, which were then plotted on a scale of zero to 2π to become independent of the heart rate interval.

To test whether the signal intensity fluctuations of the ASL images over the cardiac cycle were significantly larger than could be expected from the noise-level, a permutation test was performed where the cardiac phases were randomly reassigned to other data points before the Gaussian-weighted averaging step in the data analysis pipeline. Using the same permutations for all volunteers, the variance of the resulting signal intensity curves over the cardiac cycle ($\mathrm{Var}_{v,p}^{\mathrm{norm,\,random}}$) was calculated per permutation p and volunteer v and compared with the variance of the nonpermuted data ($\mathrm{Var}_{v}^{\mathrm{norm,card}}$). In total 600 permutations were performed. Subject-specific $\frac{\mathrm{Var}_{v,p}^{\mathrm{random}}}{\mathrm{Var}_{v}^{\mathrm{random}}}$ values were normalized according to their average over the 600 permutations allowing to pool data from all volunteers, resulting in a normalized $\mathrm{Var}_{v,p}^{\mathrm{norm,\,random}}$. Next, a distribution was built by calculating the mean normalized variance over all volunteers per permutation $\mathrm{Var}_{p}^{\mathrm{norm,random}}$, representing the normalized variances that can be expected when data points are not sorted based on their correct cardiac phase. Based on this distribution, the percentile belonging to the actual measured mean normalized variance $\overline{\mathrm{Var}_{p}^{\mathrm{norm,card}}}$ over all volunteers (i.e., using the correct cardiac phase) was calculated. The measured fluctuations were deemed to be significant if the percentile was >95% (α of 0.05).

Analogous to Li et al[8] we examined the phase dependence of the raw label/control images to be able to rule out that the fluctuations in signal are simply caused by inflow of "fresh" spins that have not experienced presaturation. Should the fluctuations be caused by inflow of fresh spins, then the raw images would exhibit the same dependence on cardiac phase, because all will be affected similarly by fresh inflow, whereas difference in label generation would not affect all raw images in the same way.

3 | RESULTS

Figure 3 shows the perfusion-weighted images for: VSArt, single-VSASL, and pCASL at 10 cardiac phase bins for a representative volunteer. Figure 4 shows the perfusion-weighted images for AccArt, single-AccArt, and pCASL for a representative volunteer. The zoomed-in part shows that VSArt, AccArt, single-AccASL, and pCASL have minimal signal in the superior sagittal sinus, the main draining vein of the brain, while single-VSASL does show some signal there. The difference between VSArt and single-VSASL indicates the expected venous labeling for single-VSASL, and shows that isolation of arterial signal in VSArt by use of pCASL as a prepulse was effective, see Figure 3. To focus on the signal variation over the cardiac cycle, the mean image over all cardiac phases was subtracted from the images; see Figures 5 and 6. The signal especially fluctuates in areas containing large arteries, which is supported by the signal intensity curves in Figure 7.

Results from the permutation test showed that the arterial signal variance over the cardiac cycle was significantly

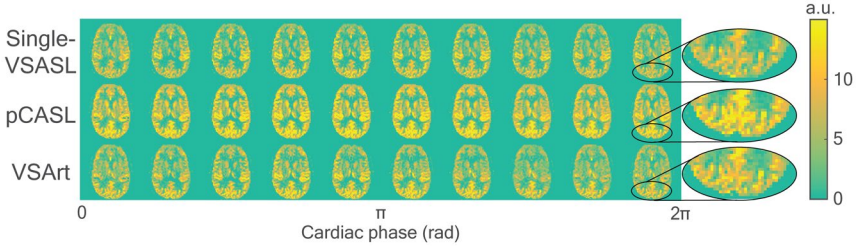

FIGURE 3 Perfusion-weighted images over the cardiac cycle of a representative volunteer for VSASL. The first row represents single-VSASL, the second row pCASL, the third row represents VSArt, i.e., the single-VSASL confined to the arterial blood pool as obtained by subtracting pCASL+VS (not shown) from regular pCASL (row 2). A zoom-in of the ellipse is shown to highlight the presence of venous signal in the sagittal sinus for single-VSASL, in contrast to pCASL, VSArt, single-AccASL, and AccArt

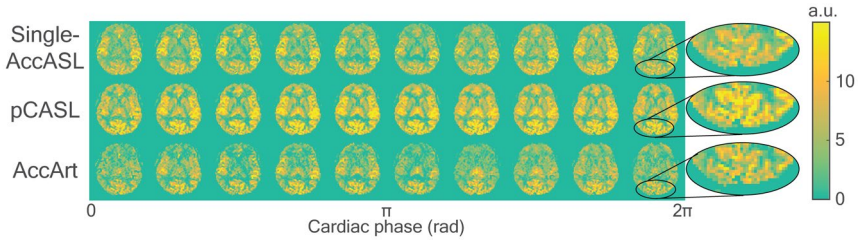

FIGURE 4 Perfusion-weighted images over the cardiac cycle of a representative volunteer for AccASL. The first row represents single-AccASL, the second row pCASL, the third row represents AccArt, i.e., the single-AccASL confined to the arterial blood pool as obtained by subtracting pCASL+Acc (not shown) from regular pCASL (row 2). A zoom-in of the ellipse is shown to highlight the absence of venous signal in the sagittal sinus for single-AccASL, pCASL, and AccArt, in contrast to single-VSASL

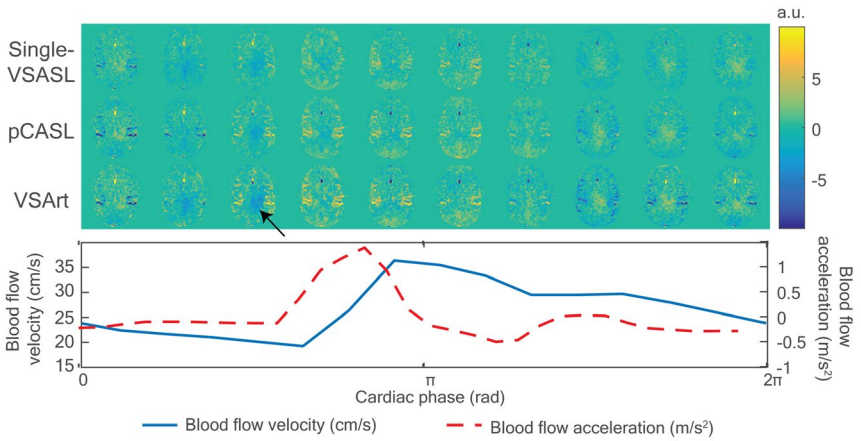

FIGURE 5 Perfusion-weighted images with the mean over the cardiac cycle subtracted for a representative volunteer for VSASL, showing the variation over the cardiac cycle with respect to the mean. Below, the corresponding blood flow velocity and acceleration are shown over the cardiac phases. Note that, in these images, negative signal means that the signal is below the average over the whole cardiac cycle. The first row represents single-VSASL, the second row pCASL, the third row represents VSArt, i.e., the single-VSASL confined to the arterial blood pool as obtained by subtracting pCASL+VS (not shown) from regular pCASL (row 2). Arrows indicate cardiac-dependent signal fluctuations in an area unrelated to perfusion, this signal is believed to stem from sub-optimal background suppression; see the Discussion section. Bottom: corresponding blood flow velocity measurement in the carotid artery, as a function of cardiac phase

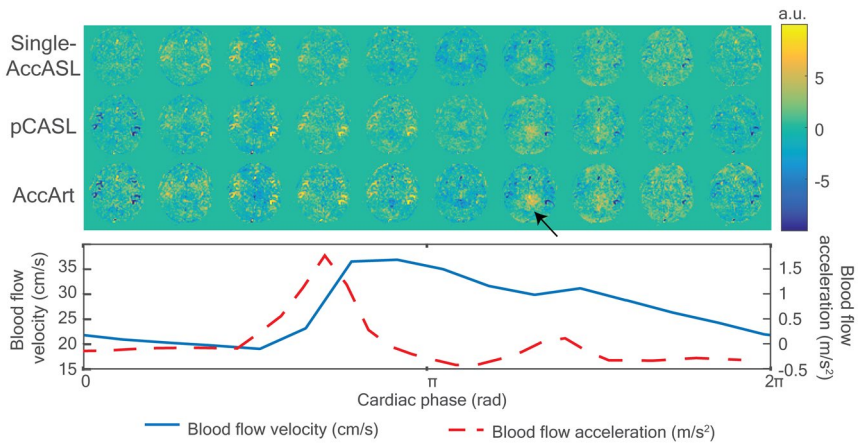

FIGURE 6 Perfusion-weighted images with the mean over the cardiac cycle subtracted for a representative volunteer for AccASL, showing the variation over the cardiac cycle with respect to the mean. Below, the corresponding blood flow velocity and acceleration are shown over the cardiac phases. Note that, in these images, negative signal means that the signal is below the average over the whole cardiac cycle. The first row represents single-AccASL, the second row pCASL, the third row represents AccArt, i.e., the single-AccASL confined to the arterial blood pool as obtained by subtracting pCASL+Acc (not shown) from regular pCASL (row 2). Arrows indicate cardiac-dependent signal fluctuations in an area unrelated to perfusion, this signal is believed to stem from sub-optimal background suppression; see the Discussion section. Bottom: corresponding blood flow velocity measurement in the carotid artery, as a function of cardiac phase

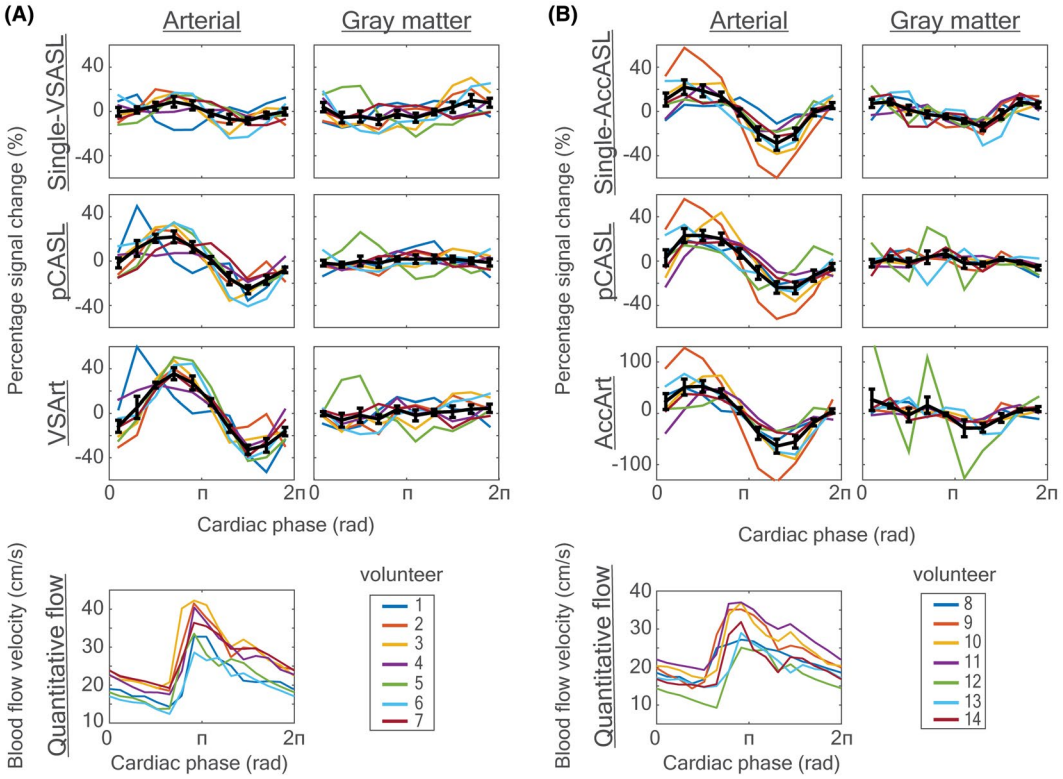

FIGURE 7 Signal intensity curves for VSASL (A) and AccASL (B), over the 10 cardiac phase bins. Left column: using arterial mask; right column: using gray matter mask. From top to bottom: the first row represents single-VSASL(AccASL), the second row pCASL, the third row represents VSArt(AccArt), i.e., the single-VSASL(AccASL) confined to the arterial blood pool as obtained by subtracting pCASL+VS(Acc) (not shown) from regular pCASL (row 2). All results are aligned according to the volunteer-specific blood velocity peak in the quantitative flow measurement, shown in the last row. Results are shown for all 7 volunteers in each group. The black line in each graph represents the mean signal over the volunteers, with error bars indicating the standard error of the mean. Note that the y-axis scale of AccArt deviates from the rest. Volunteer 12 from the AccASL-dataset showed deviating signal fluctuations in the gray matter, however, exclusion of this volunteer from the analyses, neither affected statistical findings nor changed our conclusions

higher than expected by chance in most ASL images, (VSArt $P = 0.017$, AccArt $P = 0.010$, single-AccASL $P = 0.047$, pCASL (VS dataset) $P = 0.015$ and pCASL (Acc dataset) $P = 0.024$). Within the group of volunteers in which velocity-selective labeling was applied, a signal change up to ~36% was found for VSArt, and ~26% for pCASL in the arteries. Single-VSASL did not show significant signal fluctuations over the cardiac cycle ($P = 0.202$), although a trend similar to the fluctuations of VSArt can be observed in Figure 7.

For the acceleration-selective experiments, similar results were observed, with a signal change up to ~64% for AccArt, 29% for single-AccASL, and ~24% for pCASL in arteries. Comparing the signal fluctuations with the blood flow velocity and acceleration shows that the blood flow velocity peak seems to coincide with the signal intensity peak of VSArt and pCASL, while the AccArt and single-AccASL peak is more similar to the peak in blood flow acceleration. The signal variance over the cardiac cycle in gray matter was not significantly increased.

Figure 8 shows the intensity curves of the raw label/control images before subtraction. Averaged over all volunteers, a pattern emerges; if the pCASL- and VSASL-module are both in either label or control condition, [$pCASL_{control}$ $VSASL(AccASL)_{control}$] and [$pCASL_{label}$ $VSASL(AccASL)_{label}$] the signal shows less fluctuations than if either one of them is in label condition and the other in control, [$pCASL_{label}$ $VSASL(AccASL)_{control}$] and [$pCASL_{control}$ $VSASL(AccASL)_{label}$], this is most prominently found for AccASL.

4 | DISCUSSION AND CONCLUSIONS

VSASL and AccASL are 2 promising ASL-techniques with reduced transit-time artifacts, where labeling is done based on, respectively, spin velocity and acceleration as opposed to location as done in traditional ASL. The fact that labeling is performed based upon velocity and acceleration raises the question whether the amount of label that is generated will vary over the cardiac cycle. In this study, the effect of the cardiac cycle on label generation by a *single* VSASL- and AccASL-module was investigated.

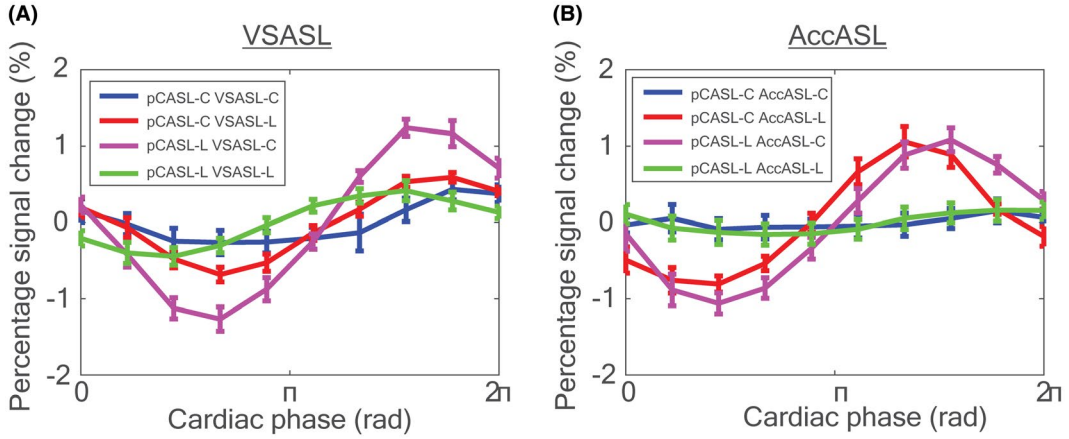

FIGURE 8 Arterial signal intensity plots of the 4 label/control images before subtraction; [$pCASL_{control}$ $VSASL_{control}$], [$pCASL_{control}$ $VSASL_{label}$], [$pCASL_{label}$ $VSASL_{control}$] and [$pCASL_{label}$ $VSASL_{label}$], of VSASL dataset (A) and AccASL dataset (B). Mean intensity averaged over all volunteers is plotted, including error bars indicating the standard error of the mean. The label/control conditions are not all influenced equally by the cardiac cycle. Cardiac cycle fluctuation is less for the conditions with both pCASL and VSASL in label or control state ([$pCASL_{control}$ $VSASL_{control}$] and [$pCASL_{label}$ $VSASL_{label}$]), as compared to the conditions where either 1 of the 2 ASL-methods is in control state ([$pCASL_{label}$ $VSASL_{control}$] and [$pCASL_{control}$ $VSASL_{label}$])

A sequence was designed to minimize cardiac-dependent effects on the signal by (1) inflow, (2) distance that the label travels into the vasculature, and (3) venous signal. Specifically, a single VSASL- or AccASL-module was combined with a pCASL preparation to limit its effect to the arterial blood pool. A short PLD was used to limit fresh inflow, and the pCASL-labeling duration was chosen longer than the average tissue transit time[10] to exclude influence of variations in the distance that label will travel into the microvasculature. Arterial label should intentionally be isolated for single VSASL(AccASL)-labeling because it also results in venous labeling, which in a regular VSASL sequence with 2 labeling modules is filtered out by the second labeling module. ASL images were retrospectively binned based on the cardiac phase during which labeling took place. Results confirm the hypothesis that VSASL(AccASL)-labeling of the arterial blood pool (VSArt/AccArt) depends on the cardiac cycle, where the AccASL signal showed higher signal fluctuations (up to 64%) than VSASL (up to 36%). In addition, pCASL (up to 25%), and single-AccASL (up to 29%) showed significant signal fluctuations over the cardiac cycle.

Effectiveness of the pCASL prepulse to isolate arterial signal is confirmed by the obtained VSArt and single-VSASL images. Single-VSASL, in contrast to VSArt, showed signal in the sagittal sinus, indicating the expected venous signal. Venous contributions can also explain why single-VSASL, in contrast to VSArt, did not show significant fluctuations over the cardiac cycle, because the venous signal will depend less on the cardiac cycle than the arterial part of the signal. Along the same lines, single-AccASL *did* show significant signal fluctuations because it has minimal venous labeling,[3] further confirmed by the AccASL images of this study, which hardly show signal in the superior sagittal sinus. However, single-AccASL still showed less signal fluctuations than AccArt, which suggests some additional signal contribution in the single-AccASL signal and possibly also in the single-VSASL signal, which is not cardiac-dependent and is filtered out using the pCASL-preparation, such as signal from diffusion-weighting caused by the VSASL- and AccASL-module.[1,3]

Results show that the peak in VSArt-signal coincides with the peak in blood flow velocity, indicating that signal fluctuations are not caused by inflow of "fresh" spins, because then an inverse relation between ASL-signal and blood flow velocity would be expected. The observations support the hypothesis that at high blood flow velocity, more spins will flow faster than the cutoff velocity(acceleration), leading to an increase in signal. As would be expected, the AccArt-signal peak coincides more with the peak in blood flow acceleration. However, difference in timing between the peak in AccArt and VSArt-signal should be confirmed by performing VSASL and AccASL experiments in the same subjects. Finally, the peak in pCASL signal also coincided with the blood flow velocity peak; note that this timing is with respect to the end of pCASL-labeling. This means that the peak in pCASL-signal might be explained by an increase in the number of spins passing through the labeling plane (and, therefore, are inverted) at end-of-labeling; moreover, this effect will be enhanced due to minimal T_1-decay for spins at end-of-labeling. However, there is also a small effect of blood flow velocity on pCASL labeling efficiency.[11]

Previous studies on the effect of the cardiac cycle on ASL have mainly focused on pulsed ASL and pCASL. Our findings confirm the general finding that cardiac influence seems to be largest in regions with large arteries.[7,8,12-14] Contrary to our results, Verbree and van Osch[15] did not

observe significant fluctuations in the pCASL signal based on the cardiac phase of end-of-labeling. This was probably due to a lack of power, because of limited averaging due to very long labeling durations and the lack of background suppression, similar to our prospectively triggered approach, described in the Supporting Information. Using the retrospectively triggered approach, more repetitions could be acquired, and a significant effect of the cardiac cycle on pCASL end-of-labeling was observed.

Li et al[8] observed increased pCASL signal instability for a nontriggered sequence compared with a triggered-sequence based on the cardiac phase during the readout excitation-pulse. Using a PLD of 1800 ms, Li et al[8] concluded that the pCASL-signal instability was most probably caused by cardiac-dependent inflow effects instead of label generation, because both label- and control-signal showed the same phase dependence over the cardiac cycle. In the current study, an effort was made to minimize inflow effects by using a shorter PLD of 500 ms, not allowing "fresh" spins to enter the imaging volume. Results show that the label/control images do not all have the same phase dependence, suggesting that the fluctuations of the signal are indeed caused by differences in the amount of label generated over the cardiac cycle, rather than inflow effects.

The images where pCASL and VSASL(AccASL) are not in the same condition; [$pCASL_{control}$ $VSASL(AccASL)_{label}$] and [$pCASL_{label}$ $VSASL(AccASL)_{control}$], show the highest cardiac dependence. This could be explained by the fact that label generation in both pCASL and VSASL are influenced by the cardiac cycle. A relatively high blood velocity at the start of the VSASL(AccASL) block leads to increased saturation by this module, so in case of the [$pCASL_{control}$ $VSASL(AccASL)_{label}$] image a relatively low signal. Similarly, for pCASL, a relatively high blood velocity at the end-of-label will lead to an increase in inverted spins at end-of-label, so a relatively low signal for [$pCASL_{label}$ $VSASL(AccASL)_{control}$]. Images where both pCASL and VSASL(AccASL) are in control-condition show less variation, indicating that there is minimal influence from inflow of 'fresh' spins from outside of the field-of-view. The image where both pCASL and VSASL(AccASL) are in label-condition also shows less cardiac dependence, which could be due to a cancellation of the 2 labeling-methods; the cardiac phase with a relatively high blood velocity, will lead to an increase in inverted spins at pCASL end-of-labeling; however, this increased inverted magnetization could in turn be saturated by the VSASL module, because more spins will have a velocity (acceleration) above the cutoff value, essentially reducing the cardiac dependence of the signal.

Some limitations should be considered when interpreting the results. Although careful consideration was given to limit confounding factors related to the cardiac cycle which might affect the data, it is possible that cardiac variations of the pCASL-signal influenced the VSArt and AccArt measurements, potentially resulting in an overestimation in the reported cardiac dependence of the VSASL and AccASL-signal. Importantly though, because VSArt(AccArt) is a subtraction of pCASL and pCASL+VS(Acc), not all of the pCASL cardiac dependence will be propagated. Specifically, all pCASL signal below the cutoff velocity(acceleration) will be subtracted out and it is expected that a large part of the bolus will be flowing below the cutoff velocity/acceleration because the pCASL labeling duration is longer than the average tissue arrival time.[10]

Another limitation of the current study is that due to the 2D-readout, later-acquired slices will effectively have a longer PLD and will not have optimal background suppression. Sub-optimal background suppression of later acquired slices have possibly resulted in the cardiac phase-dependent signal fluctuations in an area unrelated to perfusion, shown in Figures 5 and 6. The signal seems to be in anti-phase with the vascular signal and in close proximity to main CSF structures, indicated by the arrows. Both features make it likely that CSF-flow is involved in these fluctuations, but the exact origin of this signal is not completely understood. This is in accordance with a recent study which showed increased physiological noise around the ventricular system for ASL, although in that study the noise seems to be located more centrally in the brain compared with our results.[16]

In addition, the interpolation step (full width half maximum of Gaussian kernel is 18°) as well as using a PPU-device instead of electrocardiography for heart cycle recording will have introduced some smoothing of the data. The PPU could also have caused a small error in the cardiac phase if heart rate variability would have been high, because then the R-peak delay would have varied. However, heart rate variability during the scan session was found to be low (average standard deviation of RR interval = 0.11 s [VSASL] and 0.10 s [AccASL]), so we expect very minor effects on our conclusions considering the relatively low cardiac phase resolution of 10 cardiac phase bins. Lastly, it is likely that some partial volume effects will have been introduced by using arterial and gray matter masks during analysis (keeping in mind a slice thickness of 7 mm). This will have led to some overestimation of the fluctuations in the gray matter accompanied by underestimation of fluctuations in the arteries, but these effects are expected to be relatively minor.

The finding that the amount of label generated by a VSASL(AccASL)-module fluctuates over the cardiac cycle is very interesting for understanding of the technique, the interpretation and quantification of it, and for optimizing SNR. For future studies, it would be interesting to investigate how cutoff velocity(acceleration) influences the cardiac phase dependence of the VSASL and AccASL-signal. By lowering this cutoff value, the label will be created further into vascular tree, where pulsation might be decreased. However, investigating multiple cutoff velocities(accelerations) in the

current study would have come at the cost of lower SNR and/or lower resolution over the cardiac cycle, when the total examination time would be kept constant. In addition, it would also be of interest to investigate whether VSASL or AccASL could be used to measure pulsatility in the microvasculature.

The pulse wave velocity has been known to increase with age, as well as in certain diseases, such as diabetes,[17] and although the exact mechanism is still unknown, it has been associated with tissue damage in the brain.[17,18] The current view is that the brain is very susceptible to the effects of increased pulse wave velocity because of the low vascular resistance of the brain, which exposes small capillaries to high-pressure fluctuations.[17,18] The microvasculature will respond by increasing the resistance to limit the penetration of the pulsatility, but this may reduce blood flow and can lead to microscopic tissue damage.[18] Because microvascular disease is thought to be involved in strokes, dementia, and white matter lesions,[17,18] it is thus very important to be able to measure the pulsatility in the microvasculature, something which only recently has been done in smaller penetrating arteries in a single slice using phase contrast MRI at ultra-high field.[19]

In summary, this study has shown that the amount of arterial label generated by a single module of VSASL, AccASL, and pCASL can fluctuate up to 36%, 64%, and 25%, respectively, over the cardiac cycle. By acquiring sufficient averages, this effect will be averaged out. Furthermore, the presented acquisition methodology could provide an valuable starting point for future measurement of the pulsatility at the tissue level, or at least more distally in the vascular tree than is currently possible.

CONFLICT OF INTEREST

Matthias van Osch receives research support from Philips.

ORCID

Suzanne L. Franklin https://orcid.org/0000-0001-6886-5578
Matthias J. P. Osch https://orcid.org/0000-0001-7034-8959

REFERENCES

1. Wong EC, Cronin M, Wu WC, Inglis B, Frank LR, Liu TT. Velocity-selective arterial spin labeling. *Magn Reson Med*. 2006;55:1334–1341.
2. Qin Q, van Zijl P. Velocity-selective-inversion prepared arterial spin labeling. *Magn Reson Med*. 2016;76:1136–1148.
3. Schmid S, Ghariq E, Teeuwisse WM, Webb A, Van Osch M. Acceleration-selective Arterial Spin Labeling. *Magn Reson Med*. 2014;71:191–199.
4. Hernandez-Garcia L, Nielson J-F, Noll DC. Improved sensitivity and temporal resolution in perfusion fMRI using velocity selective inversion ASL. *Magn Reson Med*. 2019;81:1004–1015.
5. Wu WC, Wong EC. Feasibility of velocity selective arterial spin labeling in functional MRI. *J Cereb Blood Flow Metab*. 2007;27:831–838.
6. Wu WC, Mazaheri Y, Wong EC. The effects of flow dispersion and cardiac pulsation in arterial spin labeling. *IEEE Trans Med Imaging*. 2007;26:84–92.
7. Fushimi Y, Okada T, Yamamoto A, Kanagaki M, Fujimoto K, Togashi K. Timing dependence of peripheral pulse-wave-triggered pulsed arterial spin labeling. *NMR Biomed*. 2013;25:1527–1533.
8. Li Y, Mao D, Li Z, et al. Cardiac-triggered pseudo-continuous arterial-spin-labeling: a cost-effective scheme to further enhance the reliability of arterial-spin-labeling MRI. *Magn Reson Med*. 2018;80:969–975.
9. Golay X, Petersen ET. Pulsed star labeling of arterial regions (PULSAR): a robust regional perfusion technique for high field imaging. *Magn Reson Med*. 2005;53:15–21.
10. Liu P, Uh J, Lu H. Determination of spin compartment in arterial spin labeling MRI. *Magn Reson Med*. 2011;65:120–127.
11. Chen Z, Zhang X, Yuan C, Zhao X, Osch M. Measuring the labeling efficiency of pseudocontinuous arterial spin labeling. *Magn Reson Med*. 2017;77:1841–1852.
12. Dagli MS, Ingeholm JE, Haxby JV. Localization of cardiac-induced signal change in fMRI. *NeuroImage*. 1999;9:407–415.
13. Wu WC, Edlow BL, Elliot MA, Wang J, Detre JA. Physiological modulations in arterial spin labeling perfusion magnetic resonance imaging. *IEEE Trans Med Imaging*. 2009;28:703–709.
14. Restom K, Behzadi Y, Liu TT. Physiological noise reduction for arterial spin labeling functional MRI. *NeuroImage*. 2006;31:1104–1115.
15. Verbree J, van Osch M. Influence of the cardiac cycle on pCASL: cardiac triggering of the end-of-labeling. *MAGMA*. 2018;31:223–233.
16. Hassanpour MS, Luo Q, Simmons WK, et al. Cardiorespiratory noise correction improves the ASL signal. *Hum Brain Mapp*. 2018;39:2353–2367.
17. O'Rourke MF, Safar ME. Relationship between aortic stiffening and microvascular disease in brain and kidney: cause and logic of therapy. *Hypertension*. 2005;46:200–204.
18. Mitchel GF. Effects of central arterial aging on the structure and function of peripheral vasculature: implications for end-organ damage. *J Appl Physiol*. 2008;105:1652–1660.
19. Bouvy WH, Geurts LJ, Kuijf HJ, et al. Assessment of blood flow velocity and pulsatility in cerebral perforating arteries with 7-T quantitative flow MRI. *NMR Biomed*. 2016;29:1295–1304.

SUPPORTING INFORMATION

Additional supporting information may be found online in the Supporting Information section at the end of the article.

FIGURE S1 A, Sequence diagram for the prospectively triggered scans combining pCASL and a single VSASL- or AccASL-module. B, Pulse wave form as measured by a phase-contrast quantitative flow scan in the internal carotid artery at the level of the pCASL-labeling plane, used to calculate 5 trigger delays in the prospectively triggered scans.

One trigger delay was defined on the peak of the graph, and the rest by dividing the cardiac cycle into 5 equal parts. Using these trigger delays, the ASL images are acquired at 5 different cardiac phases

FIGURE S2 ASL images of the prospectively triggered experiments in a representative volunteer for VSASL (A) and AccASL (B), for the 5 cardiac phases. Top-row: original images, middle-row: images with the mean over cardiac cycle subtracted, note that a negative signal here means that the signal is below the mean signal over the whole cardiac cycle. Within each panel of images, the top row represents single-VSASL(AccASL), the second row pCASL, and the last row VSArt(AccArt); i.e., the arterial signal generated by the single VSASL(AccASL)-module as obtained by subtracting pCASL+VS(Acc) (not shown) from regular pCASL (row 2)

FIGURE S3 Signal intensity curves of the prospectively triggered data for VSASL (A) and AccASL (B), over the 5 cardiac phases. Left column: arterial signal as obtained by using an arterial mask; right column: gray matter signal. From top to bottom; the first row represents single-VSASL(AccASL), the second row pCASL, the third row VSArt(AccArt); i.e., the arterial signal generated by the single VSASL(AccASL)-module as obtained by subtracting pCASL+VS(Acc) (not shown) from regular pCASL (row 2). All results are aligned according to the volunteer-specific blood velocity peak in the quantitative flow measurement, shown in the last row. Results are shown for all 8 and 9 volunteers in each group, respectively. The black line in each graph represents the mean signal over the volunteers, with error bars indicating the standard error of the mean

How to cite this article: Franklin SL, Schmid S, Bos C, van Osch MJP. Influence of the cardiac cycle on velocity selective and acceleration selective arterial spin labeling. *Magn Reson Med*. 2020;83:872–882. https://doi.org/10.1002/mrm.27973